

A geometric approach to minimum-time control based on convexity

Luca Consolini[1] Oscar Gerelli[2]

Dipartimento di Ingegneria dell'Informazione - Università di Parma
Parco Area delle Scienze 181A - 43100 Parma - Italy

[1] lucac@ce.unipr.it fax +39 0521 905723 phone +39 0521 905792
[2] gerelli@ce.unipr.it fax +39 0521 905723 phone +39 0521 905716

Abstract—Starting from Pontryagin's Maximum Principle (PMP), a geometric approach is presented in order to find the optimal control for multivariable systems with input constraints. The proposed algorithm works in all the cases in which the reachable sets are convex.

The proposed approach is based on the PMP for which every optimal solution can be generated with the knowledge of two parameters: the transition time, t^* , and the final costate, q , which is the normal vector to the boundary of the set reachable at time t^* at the final state. The devised algorithm is able to find the right values of t^* and q that guarantee to reach the final state x_1 , through a geometric method that make use of the hypothesis of convexity of system reachable sets. A convergence analysis is presented and the method is validated through simulations and experiments on two sample systems: a double order integrator, for which the reachable set is also represented, and the linearized model of a flexible joint device.

I. INTRODUCTION

In many applications, such as robotic manipulators, disk-drive heads, or pointing systems, sophisticated control algorithms are required to make optimal use of the maximum torque available for rapid maneuvers, [1] [2].

In the general case the solution of minimum time problems can be formulated using the Pontryagin's Maximum Principle (PMP) but its analytical solution is quite hard to find except for simple dynamic systems. The difficulty of the problem arises because the application of PMP implies the solution of a Two Point Boundary Value Problem (TPBVP) [3] which, in general, is very difficult to solve in closed form.

A number of time-optimal bang-bang control algorithms have been proposed in the literature. One can recall the switching time variation method (STVM) [4] and the switch time optimization (STO) [5] algorithm. In all of them controls are assumed to be bang-bang, and the switching times are computed to achieve a minimum final time.

The proposed approach is based on the PMP for which every optimal solution can be generated with the knowledge of two parameters: the transition time, t^* , and the final costate, q , which is the normal vector to the boundary of the set reachable at time t^* at the final state. The devised algorithm is able to find the right values of t^* and q that guarantee to reach the final state x_1 , through a geometric method that make use of the hypothesis of convexity of system reachable sets. A proof of convergence is presented.

Partial support for this research has been provided by MIUR scientific research funds.

The paper is organized as follows. In §II the control problem is proposed and a solution is obtained in the subsequent section by means of an algorithm mainly based on the assumption of convexity of the reachable set. In §IV the dynamic model of a flexible joint is devised. It will be used in §VI for the validation of the proposed control technique, where simulations and experimental test cases are discussed. Then §VII draws the final conclusions.

Notation: For any two vectors $v, w \in \mathbb{R}^n$, $\langle v, w \rangle = \sum_{i=1}^n v_i w_i$ denotes the scalar product. Given $v \in \mathbb{R}^n$, $\hat{v} = \frac{v}{\|v\|}$ denotes the unit vector having the same direction as v . Given a set $\mathcal{A} \subset \mathbb{R}^n$, $\partial\mathcal{A}$ denotes the boundary of \mathcal{A} . The set $S^n \subset \mathbb{R}^{n+1} = \{x \in \mathbb{R}^{n+1} : \|x\| = 1\}$.

II. PRELIMINARIES

Consider a non linear system of the following general form

$$\begin{cases} \dot{x} = f(x, u) \\ x(0) = x_0 \end{cases} \quad (1)$$

where $x \in \mathbb{R}^n$, $u(t) \in \mathbb{R}^m$. It is assumed that the input function satisfies the following condition

$$u(t) \in U, \forall t \geq 0,$$

where $U \subset \mathbb{R}^m$ is an arbitrary convex set. With the notation $x_u(t)$ denote the solution of (1) for a given input function $u(t)$.

The *time-optimal problem* consists in minimizing the time needed for a transition from initial state x_0 to final state x_1

$$\min_u \{t_1 | x_u(t_1) = x_1\}, u(t) \in U, \forall t \geq 0.$$

A. Characterization of the optimal solution

One of the most important tools for optimal control is the Pontryagin's Maximum Principle (PMP), which gives a complete characterization of the optimal solutions. In the case of minimum-time problem it can be formulated as follows.

Theorem 1 (PMP): If $u(t)$ is an admissible control for system (1) that is a solution of the time-optimal problem with final time t_1 , then there exists a Lipschitz function

$$q(t) \in \mathbb{R}^n, q(t) \neq 0, \forall t \in [0, t_1]$$

such that, almost everywhere on $[0, t_1]$,

$$\begin{aligned} q^T f(x, \bar{u}) &= \max_{u \in U} q^T f(x, u), \\ \dot{q}(t) &= -q^T \frac{df}{dx} \Big|_{x=x_{\bar{u}}(t)}, \\ q^T f(x, \bar{u}) &= 0. \end{aligned} \quad (2)$$

In the case of linear systems

$$\begin{aligned} \dot{x} &= Ax + bu \\ x(0) &= x_0, \end{aligned}$$

the costate equation reduces as follows

$$\begin{aligned} \dot{q} &= -A^T q \\ q^T f(x, \bar{u}) &= \max_{u \in U} q^T Bu. \end{aligned}$$

Definition 1: The reachable set of system (1) is defined as

$$\mathcal{A}_{x_0}(t) = \{x_u(t) | u \in L^\infty([0, t], U)\}.$$

An important fact is that the final state x_1 must lie on the boundary of the reachable set from x_0 in final time t^* , i.e. $x_1 \in \partial \mathcal{A}_{x_0}(t^*)$.

B. Characterization of convexity

Definition 2: A set $C \in \mathbb{R}^n$ is convex if $\forall x, y \in C, x + \lambda(y - x) \in C, \forall \lambda \in [0, 1]$.

In differential geometry convexity can be characterized by the *shape operator* as follows,

Definition 3: Consider a $n - 1$ dimensional differentiable manifold \mathcal{M} , embedded in \mathbb{R}^n , represented by the image of the function $M : \Omega \subset \mathbb{R}^{n-1} \rightarrow \mathbb{R}^n$, i.e.

$$M = M(\Omega),$$

let $\hat{n}(x) \in S^{n-1}$ be the normal unit vector to \mathcal{M} at $M(x)$ the *shape operator* is the mapping $\mathcal{S} : \mathbb{R}^{n-1} \rightarrow \mathbb{R}^{n-1}$, such that

$$\mathcal{S}_x(v) = -\frac{d\hat{n}(x + \lambda v)}{d\lambda}.$$

The shape operator characterizes the manifold curvature as follows: let $\gamma(t) \in \mathcal{M}$ be a smooth arc-length parametrized curve such that $\gamma(0) = x$ and $\dot{\gamma} = v$, then

$$\langle \ddot{\gamma}, \hat{n}(x) \rangle = \langle v, \mathcal{S}_x v \rangle.$$

For convex manifolds the following result holds which is a direct consequence of proposition (3.2), chapter 7 of [6].

Proposition 1: If C is a convex subset of \mathbb{R}^n , then on its boundary the second fundamental form is positive semi-definite, i.e.

$$\mathcal{S}(x) \geq 0, \forall x \in \partial C. \quad (3)$$

If the manifold \mathcal{M} is not differentiable, then Definition 3 cannot be directly applied. This is exactly the case of the reachable set which in general is not differentiable, see for example figure V. In this case the concept of normal vector must be substituted with the concept of normal cone, as reported in Definition 2, chapter 5 of [7].

Definition 4: The normal cone at $x \in C$ where C is a convex subset of \mathbb{R}^n , is given by

$$N_C(x) = \{p \in C | \langle p, y - x \rangle \geq 0, \forall y \in C\}. \quad (4)$$

The shape operator cannot be defined in the usual form for non-differentiable manifold, anyway its inverse \mathcal{S}^{-1} can be defined also in this case as follows: on the boundary of convex set C define the mapping

$$x = T(q), \text{ where } q \in N_C(x),$$

which is well defined and continuous. The inverse of the shape operator is

$$\mathcal{S}_x^{-1} = \frac{dT(q)}{dq}, \text{ with } x = T(q).$$

C. Problem formulation

Definition 5: Given an initial state $x_0 \in \mathbb{R}^n$, the *final costate mapping* $\gamma_f : \mathbb{R}^n \times \mathbb{R} \rightarrow \mathbb{R}^n$, is given by

$$\gamma_f(q_1, T) = x(T),$$

where $x(t)$ is the solution at time T of the augmented system (1) + (2) with boundary conditions $x(0) = x_0$ and $q(T) = q_1$.

The *initial costate mapping* $\gamma_i : \mathbb{R}^n \times \mathbb{R} \rightarrow \mathbb{R}^n$, is given by

$$\gamma_i(q_0, T) = x(T),$$

where $x(t)$ is the solution at time T of the augmented system (1) + (2) with boundary conditions $x(0) = x_0$ and $q(0) = q_0$.

The only difference between functions γ_i and γ_f lies on the fact that the boundary conditions on the costate is given on the initial and, respectively, the final state. The relations between the two functions is given by following proposition.

Proposition 2: Let $\phi(t) \in \mathbb{R}^{n \times n}$ be the solution of system

$$\dot{\phi} = -\frac{df(x, \bar{u})^T}{dx} \Big|_{x=x_{\bar{u}}(t)} \phi,$$

where \bar{u} is given by 2, then if $q = \phi(q_0)$ it is

$$\gamma_f(q, T) = \gamma_i(q_0, T).$$

The general problem considered in this article is the following

Problem 1: Given a nonlinear system of the form (1) and a final state x_1 , find a initial costate q_0 and a time T such that

$$x_1 = \gamma_i(q_0, T)$$

III. MAIN RESULT

The basic geometric idea of the proposed algorithm is depicted in Figure 1. Given a final costate q and a final time t^* , consider the final state $x = \gamma_f(q, t^*)$. Remark that q represents the normal vector at x to the set of states reachable in time t^* . The error vector is defined as $e = x_1 - x$ and is decomposed as follows

$$e_N = \langle e, \hat{q} \rangle ; e_T = e - \langle e, \hat{q} \rangle \hat{q},$$

where e_N is the error component parallel to q and e_T is parallel to the boundary of the reachable set $\mathcal{A}_{x_0}(t^*)$ at x .

If q is varied by the small quantity δq it follows that the final state varies by

$$\delta x = S^{-1} \delta q,$$

which satisfies $\langle \delta x, \delta q \rangle \geq 0$, because of the convexity of the reachable set.

Therefore if δq is proportional to the tangential error, i.e. $\delta q = K_T e_T$, the tangential error is reduced. On the other hand the normal error can be reduced by increasing the final time t^* by a term proportional to the normal error itself, exploiting the fact that the state derivative $f(x, \bar{u})$ is always directed outwards with respect to the reachable set.

A key technical fact is that the error vector will always be inside a cone with axis q and semi-aperture $\arcsin \sqrt{1 - \beta^2}$, where β is a tuning parameter close to 1.

The following Theorem proves that using this technique the error is reduced to zero.

Theorem 2: Consider system (2), with the associated final state mapping $x_1 = \gamma_f(q, T)$. Choose $\beta \in (0, 1)$ sufficiently close to 1 such that

$$\frac{\beta}{1 - \beta^2} > \max_{\mathcal{A}_0(T)} \|f(x, u)\|, \quad (5)$$

define the error function as $e(q, t) = x_f - S(q, t)$ and consider the following differential system

$$\begin{aligned} \frac{dT}{d\lambda} &= \frac{K_T(1-\beta)}{\beta} \langle e, q \rangle \\ \frac{dq}{d\lambda} &= K_T(e - \langle e, \hat{q} \rangle \hat{q}), \end{aligned} \quad (6)$$

then if the reachable sets $\mathcal{A}_{x_0}(T)$ are convex for all $T \geq 0$ and if

$$\langle \hat{e}(0), \hat{q}(0) \rangle > \beta, \quad (7)$$

then

$$\langle \hat{e}(t), \hat{q}(t) \rangle > \beta, \forall t \geq 0. \quad (8)$$

moreover it is

$$\lim_{\lambda \rightarrow \infty} e(\lambda) = 0. \quad (9)$$

Proof: Equation (8) is equivalent to

$$\langle e, \hat{q} \rangle - \beta \|e\| \geq 0, \forall t \geq 0,$$

deriving the above expression,

$$\begin{aligned} \frac{d \langle e, \hat{q} \rangle - \beta \|e\|}{d\lambda} &= \\ &= \langle \dot{e}, \hat{q} \rangle + \langle e, \dot{\hat{q}} \rangle - \beta \langle \dot{e}, \hat{e} \rangle, \end{aligned} \quad (10)$$

where the dot denotes the derivatives with respect to λ .

Rewrite these three terms taking into account (6)

$$\begin{aligned} \langle \dot{e}, \hat{q} \rangle &= -\frac{K_T(1-\beta)}{\beta} \langle f, \hat{q} \rangle \langle e, \hat{q} \rangle \|q\| = \\ &= -\frac{K_T(1-\beta)}{\beta} \langle e, \hat{q} \rangle, \end{aligned}$$

where it has been used the fact that $\langle f, q \rangle = 1$, moreover

$$\langle e, \dot{\hat{q}} \rangle = \langle e, K_T(e - \langle e, \hat{q} \rangle \hat{q}) \rangle = K_T \|e\|^2 (1 - \langle \hat{e}, \hat{q} \rangle^2),$$

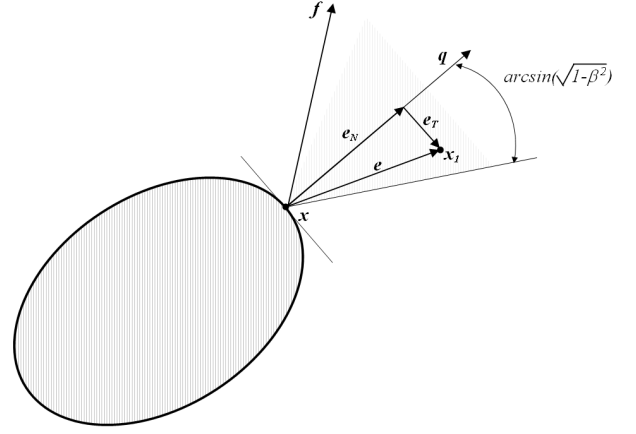


Fig. 1. A schematic representation of the control technique.

$$\begin{aligned} -\beta \langle \dot{e}, \hat{e} \rangle &= -\beta \left(\frac{K_T(1-\beta)}{\beta \|f\|} \langle f, \hat{e} \rangle \langle e, \hat{q} \rangle + \right. \\ &\quad \left. + K_T \langle e - \langle e, \hat{q} \rangle \hat{q}, S^{-1}(e - \langle e, \hat{q} \rangle \hat{q}) \rangle \right) \end{aligned}$$

where S^{-1} is the inverse shape operator of the boundary of the reachable set in the last expression, it is $\langle f, \hat{e} \rangle \geq 0$, in fact $\langle f, \hat{e} \rangle = \langle f_q, \hat{e} \rangle + \langle f_q^\perp, \hat{e} \rangle \geq \beta - \|f\|(1 - \beta^2) > M$, moreover, being the border of the reachable set convex, matrix S is negative definite, therefore

$$-\beta \langle \dot{e}, \hat{e} \rangle \geq M \|e\| \langle e, \hat{q} \rangle,$$

and equation (10) can be bounded as follows

$$\begin{aligned} \frac{d \langle e, \hat{q} \rangle - \beta \|e\|}{d\lambda} &\geq \\ &\geq K_T \|e\|^2 (1 - \langle e, \hat{q} \rangle^2) - \frac{(1-M)(1-\beta)^2}{\beta} \langle \hat{e}, \hat{q} \rangle \end{aligned}$$

evaluating this expression for $\langle \hat{e}, \hat{q} \rangle = \beta$ it follows that

$$\begin{aligned} \frac{d \langle e, \hat{q} \rangle - \beta \|e\|}{d\lambda} &\geq \\ &\geq K_T \|e\|^2 \left(1 - \beta^2 - \frac{(1-M)(1-\beta)^2}{\beta} \right) \geq 0 \text{ if } \|e\| \geq 0, \end{aligned}$$

therefore (8) must hold.

Consider now the equation for normal error $\langle e, \hat{q} \rangle$, it is $\frac{d}{d\lambda} \langle e, \hat{q} \rangle = \langle \dot{e}, \hat{q} \rangle + \langle e, \dot{\hat{q}} \rangle$, which corresponds to the first two terms of (10) and it follows that

$$\begin{aligned} \frac{d}{d\lambda} \langle e, \hat{q} \rangle &= \\ &= -\frac{K_T(1-\beta)^2}{\beta} \langle f, q \rangle \langle e, q \rangle + K_T \|e\|^2 [1 - \langle e, \hat{q} \rangle^2] \leq \\ &\leq -\|e\|^2 \langle \hat{e}, \hat{q} \rangle K_T [(1-\beta^2) + (1-\beta)] \leq \\ &\leq -\|e\|^2 \langle e, \hat{q} \rangle K_T \left[\frac{(1-\beta)}{\beta} \right] \\ &\leq -\langle e, \hat{q} \rangle^3 \frac{K_T}{(1+\beta)\beta}. \end{aligned}$$

Therefore by the comparison lemma

$$\lim_{\lambda \rightarrow \infty} \langle e, q \rangle = 0,$$

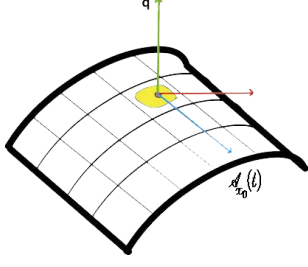


Fig. 2. The reachable set $\mathcal{A}_{x_0}(t)$

and, being by (8) $\|e\| \leq \| \langle e, \hat{q} \rangle \| \sqrt{1+\beta^2}$, the thesis (9) follows. ■

Remark 1: Theorem 2 represents a procedure that can be used for the computation of the time-optimal control for systems whose accessibility sets are convex. The convexity is crucial because allows the inverse of the shape operator S to be semidefinite positive. The property of convexity is enjoyed by various kind of systems, for example linear time-varying systems, some bilinear systems [8], nonlinear systems with small inputs [9].

Remark 2: Satisfying condition (5) may represent a problem, because it requires an a priori estimate of the reachable set passing at the final state, x_1 . In practice, if the algorithm does not converge, the term $1 - \beta$ can be reduced until convergence is obtained.

IV. FLEXIBLE JOINT MODEL

To experimentally validate the algorithm in §III, a flexible joint system has been used. The one considered in this paper is an educational mechatronic device designed by Quanser Consulting. Fig. 3 shows the top view of the experimental device: a rigid arm is connected, through a flexible joint, to a rotating “body”, which is actuated by a servo motor. Both the body and the arm can rotate around vertical axis “ O ” of Fig. 3. The elastic coupling between the body and the arm is obtained by means of two springs whose stiffness is K_e and whose unstretched length is l_0 .

Since the described control technique is based on the knowledge of the system model, an accurate nonlinear model, mainly used for simulation purposes, is proposed in the following. The linearized version of the same model, to be used for the controller synthesis, is then devised.

Spring forces f_1 and f_2 cover an important role in the system dynamics. In order to evaluate their amplitude, let us assign a reference frame $\{1\}$ whose origin is located in “ O ” and integral with the body. Moreover, let us assign a further frame $\{2\}$, located in “ O ” but integral with the arm, and indicate by θ_2 the joint angle between the two frames. Angle θ_2 is counterclockwise positive. In the same way, let us indicate by θ_1 the counterclockwise positive joint angle between the body frame $\{1\}$ and a given stationary frame.

The three points “ A ”, “ B ”, and “ C ” shown in Fig. 3 can be described with respect to frame $\{1\}$ by means of three vectors $p_a := [-d_m \ h]^T$, $p_b := [d_m \ h]^T$, and $p_c := [-R \sin \theta_2 \ R \cos \theta_2]^T$ where d_m , h , and R are the geometrical dimensions reported in the same figure.

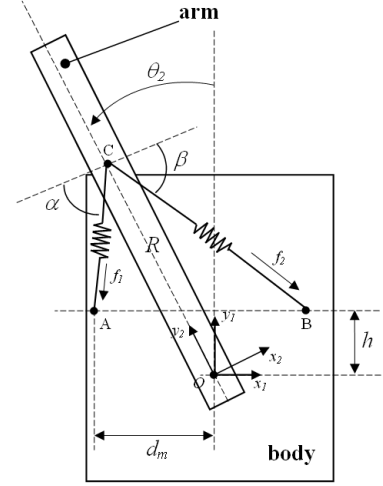


Fig. 3. Flexible joint experiment: Top view.

The spring force norms, i.e., $f_1 := \|f_1\|$ and $f_2 := \|f_2\|$, depend on the spring lengths l_1 and l_2 according to equations

$$f_1 = K_e(l_1 - l_0), \quad (11)$$

$$f_2 = K_e(l_2 - l_0), \quad (12)$$

where l_1 and l_2 can be evaluated as follows

$$l_1 = \frac{\|p_c - p_a\|}{\sqrt{R^2 + d_m^2 + h^2 - 2R(d_m \sin \theta_2 + h \cos \theta_2)}}, \quad (13)$$

$$l_2 = \frac{\|p_c - p_b\|}{\sqrt{R^2 + d_m^2 + h^2 + 2R(d_m \sin \theta_2 - h \cos \theta_2)}}. \quad (14)$$

Forces acting on point “ C ” can be described with respect to frame $\{2\}$ leading to

$$\begin{bmatrix} f_{1_x} \\ f_{1_y} \end{bmatrix} = \begin{bmatrix} f_1 \cos(\alpha) \\ f_1 \sin(\alpha) \end{bmatrix} = \begin{bmatrix} -K_e(l_1 - l_0) \cos(\alpha) \\ -K_e(l_1 - l_0) \sin(\alpha) \end{bmatrix}$$

and

$$\begin{bmatrix} f_{2_x} \\ f_{2_y} \end{bmatrix} = \begin{bmatrix} f_2 \cos(\beta) \\ f_2 \sin(\beta) \end{bmatrix} = \begin{bmatrix} K_e(l_2 - l_0) \cos(\beta) \\ -K_e(l_2 - l_0) \sin(\beta) \end{bmatrix}$$

where $\alpha, \beta \in \mathbb{R}^+$ are the two auxiliary angles shown in Fig. 3 which can be evaluated by means of the following equations

$$\alpha(\theta_2) = \arctan \left[\frac{R \cos(\theta_2) - h}{d_m - R \sin(\theta_2)} \right] - \theta_2,$$

$$\beta(\theta_2) = \arctan \left[\frac{R \cos(\theta_2) - h}{d_m + R \sin(\theta_2)} \right] + \theta_2.$$

Elastic forces induce an elastic nonlinear torque in the arm that can be expressed as

$$\tau_e = [-f_{1_x}(\theta_2) - f_{2_x}(\theta_2)] R.$$

It is worth noting that components f_{1_y} and f_{2_y} do not generate any torque with respect to “ O ”.

It is now possible to propose the dynamic equation of the rigid arm described with respect to “ O ”

$$J_{load}(\ddot{\theta}_2 + \ddot{\theta}_1) = [-f_{1_x}(\theta_2) - f_{2_x}(\theta_2)] R - B_{eq}^L \dot{\theta}_2 \quad (15)$$

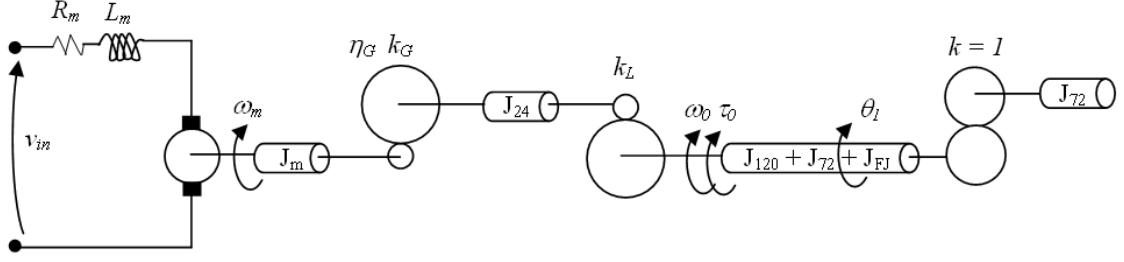


Fig. 4. Inertia and gearboxes ratio chain view from motor rotor axis

where J_{load} is the arm inertia evaluated with respect to “O”, while B_{eq}^L is the friction coefficient associated to angular velocity $\dot{\theta}_2$. Practically, arm dynamics takes into account torques which are due to inertia, friction and elasticity.

Similarly, it is possible to devise the dynamic equation of the “body”. It is made of an inertial load joined to an electric motor by means of a chain of reduction gears according to the scheme shown in Fig. 4. Even in this case, the system is affected by torques deriving from inertia, friction and elasticity

$$J_{eq}^0 \ddot{\theta}_1 = \tau^0 - B_{eq}^0 \dot{\theta}_1 - [-f_{1x}(\theta_2) - f_{2x}(\theta_2)] R + B_{eq}^L \dot{\theta}_2, \quad (16)$$

where J_{eq}^0 is the equivalent inertia of the system composed by motor, reduction gears, and “body”, τ^0 is the motor torque, while B_{eq}^0 is the friction coefficient associated to angular velocity $\dot{\theta}_1$. All the quantities in (16) are referred to the output shaft of the system. For a system like that shown in Fig. 4 the equivalent inertia can be expressed as

$$J_{eq}^0 = [J_m k_g^2 k_l^2 \eta_g + J_{24} k_l^2 + J_{120} + 2J_{72} + J_{FJ}]$$

where k_g and k_l are gearbox reduction rates, J_{24} , J_{72} , and J_{120} are gearboxes inertias, J_{FJ} is the body inertia, J_m is the motor inertia, while η_g represents the efficiency of the motor gearbox.

Output torque τ_0 depends on the motor characteristics and on characteristics of the power train. It is possible to verify that it can be expressed as

$$\tau^0 = \frac{k_g k_l k_m \eta_g \eta_m}{R_m} v_{in} - \frac{k_g^2 k_l^2 k_m^2 \eta_g \eta_m}{R_m} \dot{\theta}_1 \quad (17)$$

where η_m is the motor efficiency, k_m is the motor electric constant, R_m is the motor winding resistance, and v_{in} is the motor feeding voltage.

Bearing in mind (17), it is possible to rewrite (16) as follows

$$J_{eq}^0 \ddot{\theta}_1 = -G \dot{\theta}_1 + B_{eq}^L \dot{\theta}_2 - [-f_{1x}(\theta_2) - f_{2x}(\theta_2)] R + H v_{in}, \quad (18)$$

where

$$G = \frac{k_g^2 k_l^2 k_m^2 \eta_g \eta_m}{R_m} + \beta_{eq}^0, \quad (19)$$

$$H = \frac{k_g k_l k_m \eta_g \eta_m}{R_m}. \quad (20)$$

Equations (15) and (18) represent the complete nonlinear dynamic model of the flexible joint system and are used

to simulate the system behavior. For the synthesis of the control technique proposed in §II an equivalent linear model is devised. Elastic torque τ_e is the sole nonlinear term which appears in (15) and (18). It can be linearized in $\theta_2 = 0$ leading to $\tau_e \simeq -K_{stiff} \theta_2$, where K_{stiff} is an equivalent stiffness constant. Consequently, (15) and (18) can be rewritten as

$$J_{eq}^0 \ddot{\theta}_1 = -G \dot{\theta}_1 + B_{eq}^L \dot{\theta}_2 + K_{stiff} \theta_2 + H v_{in} \quad (21)$$

$$J_{load} (\ddot{\theta}_2 + \dot{\theta}_1) = -B_{eq}^L \dot{\theta}_2 - K_{stiff} \theta_2. \quad (22)$$

Finally, it is possible to rewrite (21) and (22) into a state-space form $\dot{x} = Ax + b v_{in}$ by assuming $x := [x_1 x_2 x_3 x_4]^T = [\theta_1 \theta_2 \dot{\theta}_1 \dot{\theta}_2]^T$ and defining

$$A = \begin{bmatrix} 0 & 0 & 1 & 0 \\ 0 & 0 & 0 & 1 \\ 0 & \frac{K_{stiff}}{J_{eq}^0} & -\frac{G}{J_{eq}^0} & \frac{B_{eq}^L}{J_{eq}^0} \\ 0 & -\frac{K_{stiff}(J_{load} + J_{eq}^0)}{J_{load} J_{eq}^0} & \frac{G}{J_{eq}^0} & -\frac{B_{eq}^L(J_{load} + J_{eq}^0)}{J_{load} J_{eq}^0} \end{bmatrix} \quad (23)$$

$$b = \begin{bmatrix} 0 \\ 0 \\ \frac{H}{J_{eq}^0} \\ -\frac{H}{J_{eq}^0} \end{bmatrix}. \quad (24)$$

V. NUMERICAL IMPLEMENTATION

The approach devised in §III has been implemented in software by means of the Algorithm 1.

The input parameters are the following: $K_T \in \mathbb{R}^+$ is a gain term of the error function, x_1 is the final state, ε_e represent the error tolerance and β is a tuning parameter that must be close to 1 (see Remark 2). Moreover $\phi(q, t) \in \mathbb{R}^{n \times n}$ is the solution of

$$\begin{aligned} \dot{\phi} &= -\frac{df(x, \bar{u})^T}{dx} \Big|_{x=x_{\bar{u}}(t)} \phi \\ \phi(0) &= I \end{aligned}$$

where f is the system function, $x \in \mathbb{R}^n$ is the state-vector and \bar{u} is found with (2).

The algorithm is a direct application of Theorem 2. In particular equation (6) is solved using the initial state $t(0) = 0$ and $q = q_0(0) = x_1$, such that $\langle \hat{e}(0), \hat{q}(0) \rangle = 1$, and (7) holds.

The algorithm ends when the norm of the error between the final state x_1 and the current state $\gamma_i(q_0, t^*)$ is less than the tolerance ε_e .

Remark that the Euler algorithm is used here only for simplicity, but any kind of differential equation solver can be adopted, i.e. Runge-Kutta method.

Algorithm 1: MTC

Compute the minimum-time feedforward control.

input : $x_1, \varepsilon_e, \beta, K_T$

output: q_f and t^*

begin

$t_0 = 0;$

$q_0 = 0;$

while $e \leq \varepsilon_e$ **do**

$(\frac{dT}{d\lambda}, \frac{dq}{d\lambda}) \leftarrow G(\hat{q}_0, t);$

$\hat{q}_0 \leftarrow \hat{q}_0 + \phi(q, t)^{-1} \frac{dq}{d\lambda};$

$t \leftarrow t + \frac{dT}{d\lambda};$

$q_f \leftarrow \phi(q, t)\hat{q}_0;$

$t^* = t;$

$u^*(t) \leftarrow \text{sgn}(q_f B);$

end

Algorithm 2: $G(q, t)$

Solve the external differential equation.

input : t and q

output: $\frac{dT}{d\lambda}$ and $\frac{dq}{d\lambda}$

begin

$\tilde{x}_1 \leftarrow S(q, t);$

$e \leftarrow \|x_1 - \tilde{x}_1\|;$

Compute $\phi(\hat{q}_0, t);$

$\frac{dT}{d\lambda} \leftarrow \frac{K_T(1-\beta)}{\beta} \langle e, q \rangle;$

$\frac{dq}{d\lambda} \leftarrow K_T(e - \langle e, \hat{q} \rangle \hat{q});$

end

VI. SIMULATION AND EXPERIMENTAL RESULTS

Two different type of systems have been used to evaluate the correctness and the convergence of the proposed approach. Simulations have been performed under Matlab environment, while experimental results have been conducted thanks to the interaction between Matlab and WinCon real-time extension.

First of all the algorithm has been tested with a dummy problem, a double order integrator system. Then simulations and experimental results have been carried on the linearized model of the flexible joint system described in §IV.

A. Double order integrator

A double order integrator is one of the simplest time-invariant systems in control issues, it is given by

$$\begin{cases} \dot{x}_1 = x_2 \\ \dot{x}_2 = u \end{cases},$$

the related state space representation is $\dot{x} = Ax + Bu$, where



Fig. 5. The reachable set at $t_f^* = 1$ s for the double order integrator

$$A = \begin{bmatrix} 0 & 1 \\ 0 & 0 \end{bmatrix} \quad b = \begin{bmatrix} 0 \\ 1 \end{bmatrix}. \quad (25)$$

The reachable set $\mathcal{A}_0(1) = \gamma_i(S^1, 1)$ is shown in figure V: the set is convex, with two non-differentiable points respectively in $x = [-2.5, -5]^T$ and $x = [2.5, 5]^T$.

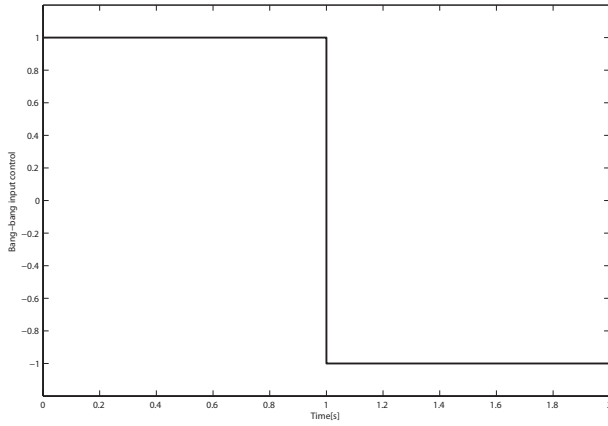
The control law that corresponds to the final state $x = [1, 0]^T$ has been computed considering the input constraint $\|u(t)\|_\infty \leq 1$ so that $U = [-1, +1]$. Simulation results are shown in Figure 6. As expected the input control is a standard bang-bang signal; in the first half of the optimal transition the system accelerates at the maximum rate and then it decelerates, always at the maximum admissible rate, to get to the desired final state.

B. Flexible joint system

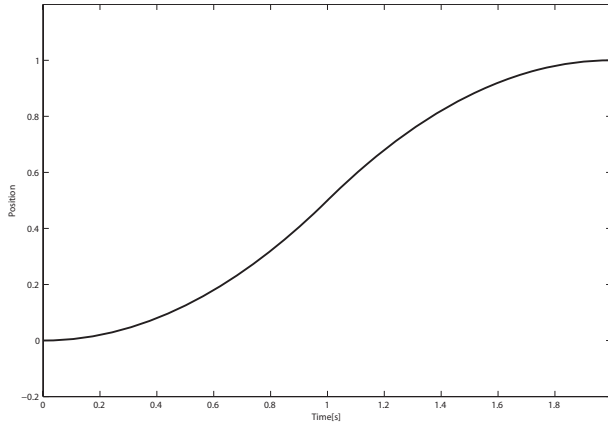
By substituting flexible joint parameters in state space model, described by equation (23) and (24), the experimental plant can be represented by a linearized system $\dot{x} = Ax + Bu$, where

$$A = \begin{bmatrix} 0 & 0 & 1 & 0 \\ 0 & 0 & 0 & 1 \\ 0 & 379.9 & -56.65 & 2.956 \\ 0 & -512.9 & 56.65 & -3.99 \end{bmatrix} \quad b = \begin{bmatrix} 0 \\ 0 \\ 93.74 \\ -93.74 \end{bmatrix}.$$

Time-optimal feedforward control $\bar{u}(t)$ has been obtained with the algorithm described in §V, to get a rest-to-rest transition from $y = 0$ to $y = \pi/4 (= y_f)$. Since the maximum bidirectional output voltage of the amplifier used to control the flexible joint is equal to 5 Volts, the input constraint is given by $\|u(t)\|_\infty \leq 5$, so that $U = [-5, +5]$. The optimal transition is performed in $t_f^* = 0.31$ s and the related control signal is reported in Figure 7. Figure 7(b) shows the comparison between the simulated plant output and the real one. Since the proposed approach has been tested on the linearized model of the flexible joint, the behavior difference is mainly due to friction and other neglected system non-linearities.



(a) Bang-bang input control



(b) System output

Fig. 6. Simulation of a double order integrator subject to input constraint for a transition to final state $\mathbf{x} = [1 \ 0]^T$.

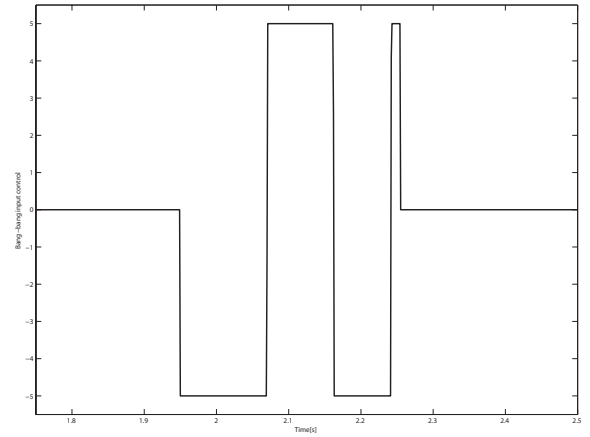
As validation of the correctness of the devised solution, this result has been successfully compared with the one obtained by the algorithm described in [10].

VII. CONCLUSIONS

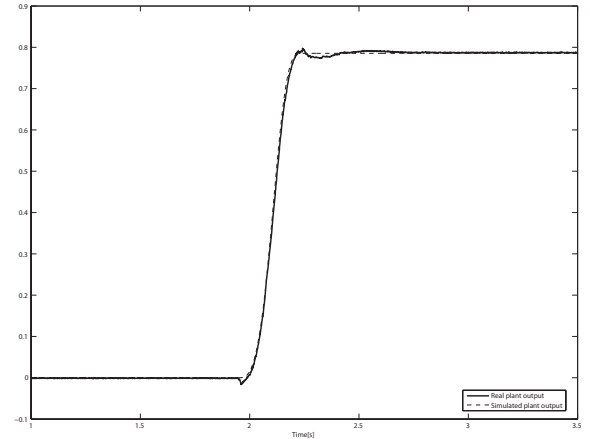
The paper has proposed a geometric invariant approach in time-optimal control for an input constrained transition. The algorithm is based on the convexity of the reachable set, so it is useful for all those systems whose reachable set is convex, such as linear systems. This control technique applies also for some type of bi-linear systems. A proof of convergence for the proposed method has been devised and experimental results has been successfully shown for two different plants.

REFERENCES

- [1] K. S. Anantharayanan, "Third-order theory and bangbang control of voice coil actuators." *IEEE Trans. Magnetics*, 1982.
- [2] R. S. B. Wie and Q. Liu, "Robust time-optimal control of uncertain structural dynamic systems." *AIAA J. Guid. Control Dyn.*, 1993.
- [3] C. Fotouhi and W. Szyszkowski, "A numerical method for time optimal control of planar double arms robot." *IEEE Tr. Automatic Control*, 1996.
- [4] R. Mohler, *Nonlinear Systems*. Prentice Hall, 1991.
- [5] E. Meier and A. Bryson, "Efficient algorithm for time-optimal control of a two-link manipulator," *Journal of Guidance, Control, and Dynamics*, vol. 13, pp. 859–866, 1990.



(a) Bang-bang input control



(b) Expected system output y (dashed line) and measured plant output (solid line)

Fig. 7. Experimental results of the control technique applied to the linearized model of a rotary flexible joint subject to input constraint for a rest-to-rest transition to final state $\mathbf{x} = [\pi/4, 0, 0, 0]^T$.

- [6] M. Spivak, *A Comprehensive Introduction to Differential Geometry*. Perish, 1979.
- [7] A. C. J.P. Aubin, *A Series of Comprehensive Studies in Mathematics*. Springer-Verlag, 1979.
- [8] M. V. Topunov, "The reachable set of a quasi-commutative bilinear system: Its convexity," *Automation and Remote Control*, 2003.
- [9] B. Polyak, "The convexity principle and its applications," *Bulletin of the Brazilian Mathematical Society*, 2003.
- [10] L. Consolini and A. Piazzzi, "Minimum-time feedforward control with input an output constraints," in *Proceedings of the 2006 IEEE Computer Aided Control Systems Design Conference*, Munich, Germany, October 2006.